Photoreduction of a Crystalline Au(III) Complex: a Solid-state Approach to Metallic Nanostructures

Andreas Taubert,[†,*] Itamar Arbell, Almut Mecke and Philipp Graf

Department of Chemistry, University of Basel, Klingelbergstrasse 80, CH-4056 Basel, Switzerland.
[†] Current address: Institute of Chemistry, University of Potsdam, D-14476 Golm, Germany and Max-Planck-Institute of Colloids and Interfaces, D-14476 Golm, Germany.
* Corresponding author: Institute of Chemistry, University of Potsdam, Karl-Liebknecht-Str. 24-25, Building 26, D-14476 Golm, Germany.
Email: ataubert@uni-potsdam.de
Tel.: ++49 (0)331 977 5773.

Abstract

Gold platelets with a nanometer thickness and a width of up to 15 μm have been fabricated by photoreduction of Au(III) within a layered, crystalline gold complex. Particle shape selection (large spheres vs. platelets) is largely controlled by the sample temperature, which varies with the UV lamp-sample distance: at short distances the sample melts and only micrometer-sized spheres form, at intermediate distances platelets and spheres form, and at distances over ca. 40 cm, mostly platelets form. The particles can be stabilized with thiols and extracted from the organic matrix.

Introduction

Inorganic particles, especially gold particles,[1] are probably one of the most intensely researched fields in chemistry today. Classical procedures for inorganic particle synthesis include vapor phase reactions and wet chemistry in water and organic solvents. Recently, also ionic liquids (ILs) have been used to fabricate well-defined inorganic particles.[2, 3] Moreover, the pyridinium and imidazolium cations of ILs can coordinate to MX_4^{2-} (M = Co, Ni, Cu, Zn, Cd, Pd and X = Cl, Br) complex ions and form ionic liquid crystals (ILCs).[4-11] Because these ILCs contain a metal center and have a high degree of order, they are prime candidates for the synthesis of inorganic nanostructures. As the first example, our group has recently fabricated a macroporous network of CuCl platelets from a Cu-containing ILC. As these ILCs serve as precursors for inorganic matter, we have termed them ionic liquid crystal precursors, ILCPs.[12, 13] Unlike conventional precursor/solvent/reactant mixtures, ILCPs are "all-in-one" reactant-solvent-templates.[3, 12, 13] Other research groups have recently adapted this concept and presented their own ILCPs.[14-16]

The current paper shows that not only mesophases (i.e. ILCs) but also *crystalline* ILC analogs can template inorganic particles. Specifically, we show that dodecylpyridinium tetrachloroaurate is a precursor for the formation of gold platelets with a nanometer thickness and a micrometer width. The fabrication of inorganic particles from a crystalline metal complex precursor is a new concept that could be useful for many other inorganic materials, especially metallic nanostructures. Indeed, Chen et al. have recently shown that the controlled thermolysis of a silver thiolate yields uniform silver nanodisks.[17]

Experimental

Metal complex synthesis

Dodecylpyridinium chloride (Fluka) was recrystallized three times from THF (Aldrich) yielding a white powder. 284.5 mg of dodecylpyridinium chloride and 398 mg of $NaAuCl_4$ (Aldrich) were dissolved in 15 mL of water and vigorously stirred at room temperature (Scheme 1). A bright yellow precipitate appeared immediately and the suspension was stirred in the dark for another 30 min. to complete the reaction. The precipitate was filtered, washed with cold water, and dried under vacuum for 12 hours. The resulting complex **1** is soluble in THF, dioxane, and acetonitrile, but insoluble in water, chloroform, and toluene. ^{1}H-NMR (400 MHz, DMSO-d6, TMS) δ 0.84 (t, 3H), 1.24 (broad, 18 H, J), 1.90 (m, 2H), 4.61 (m, 2H), 8.15 (m, 2H), 8.58 (m, 1H), 9.15 (d, 2H). ^{13}C NMR (400 MHz, DMSO-d6, TMS) 146.4, 145.7, 128.9, 67.9, 61.5, 41.0, 40.8, 40.6, 40.4, 39.8, 32.2, 31.7, 29.9, 29.8, 29.7, 29.6. MS (FAB, Finnigan MAT 312) 248 (M+, ligand), 93, 80, 43. FTIR (Shimadzu FTIR 8300 with a Golden Gate ATR unit, neat samples, 2 cm^{-1} resolution) 3122, 3080, 3055, 2960, 2916, 2850, 1629,

1498, 1478, 1469, 1377, 1321, 1176, 1162, 1060, 1026, 956, 781, 717, 688 cm⁻¹. Elemental analysis calculated (%): C 34.71, H 5.31, Au 33.49, Cl 24.11, N 2.38; found: C 34.74, H 5.35, Cl 24.21, N 2.35.
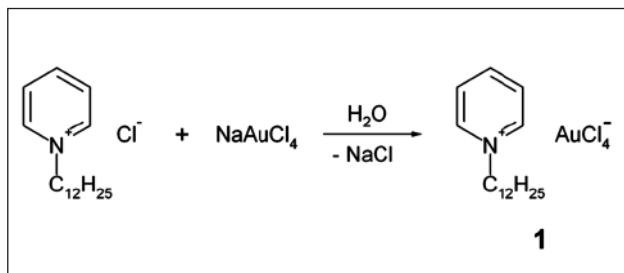
Scheme 1
Synthesis of the Au complex 1

Gold platelet synthesis

Photoreduction of **1** was done with a homebuilt UV setup with a 400 W Heraeus Nobelight broadband Hg lamp. Samples were irradiated for 60, 90, and 120 minutes at room temperature at various distances. Gold particles were extracted from the organic matrix as follows: 100 mg of the irradiated sample were suspended and stirred in doceanethiol/THF (50% v/v) for 24 hours at room temperature. The resulting golden brown precipitate was centrifuged and after repeated washing with toluene a dark red to purple solid was obtained.

X-ray diffraction

XRD measurements were done on a Siemens D5000 diffractometer with a graphite monochromator using CuKα radiation. Measurements were made from 1 to 90 degrees 2θ at a step size of 0.1 degrees/min. Single crystal analysis has failed until now due to imperfect crystals.

Differential scanning calorimetry

DSC experiments were made on a Perkin-Elmer DSC6 from 0 to 200°C at a heating rate of 10°C/min. Calibration was done with indium and lead.

Microscopy

Optical microscopy was done on a Leica DM-RP with hotstage and 10x, 20x, and 40x objectives. Scanning electron microscopy was done on a Philips XL30 FEG ESEM and a Hitachi S4800 FESEM operated at 10 and 5 kV, respectively. Samples were not sputtered for SEM imaging. Transmission electron microscopy was done on a Philips Morgagni operated at 80 kV. Atomic force microscopy was done on a Molecular Imaging PicoLE System equipped with a multi-purpose scanner. The samples were prepared by applying approximately 5 µl of sample solution onto a 2 cm x 2 cm glass cover slip and letting it air dry in the dark. Images were acquired using a silicon cantilever (type NCHR pointprobe-plus, force constant 42 N/m as given by the manufacturer for non-contact mode images or type FM point probes, force constant ~1.2-3.5 N/m as given by the manufacturer for

contact mode images; both from NanoAndMore GmbH, Wetzlar, Germany). Samples were imaged directly after drying and after various irradiation times using both contact and non-contact modes.

Spectroscopy

UV/Vis spectroscopy was done on a Safas 2000 UV/Vis spectrometer. Films of **1** were deposited from THF on a quartz UV cuvette and dried at room temperature in the dark. After recording the UV spectra of the dry solid film of **1**, the cuvette was exposed to UV light for 60 min. and the same film was measured after photoreduction of Au(III) to Au(0).

Results and discussion

Gold platelet precursor

Structurally, the complex **1** is an Au(III) analog of the many 3d and 4d metal alkylpyridinium complexes reported in the literature[4-8, 18] which are crystalline at room temperature and show thermotropic liquid crystal behavior. Like these compounds, **1** is crystalline at room temperature. X-ray-diffraction (Figure 1) shows a set of peaks that can be indexed as the 100, 200, 300, ... reflections of a layered crystal with a layer spacing of 15.5 Å.

Simple estimation of the length of the alkylpyridinium ligand shows that the dodecylpyridinium ligand is ca. 19.3 Å long. This implies that the layer spacing in the complex is too small to accommodate the ligand molecules perpendicular to the layer plane. We thus suggest that the layers consist of tilted dodecylpyridinium molecules with an estimated tilting angle of ca. 36 degrees with respect to the layer normal, similar to 3d metal ILCs.[5-8] The smaller layer spacing in our complex (15.5 Å vs. 17.2 Å in the Cu analog) is assigned to the fact that the corresponding Cu complex contains two ligand molecules per formula unit,[8] whereas the gold complex **1** only contains one ligand per metal ion.
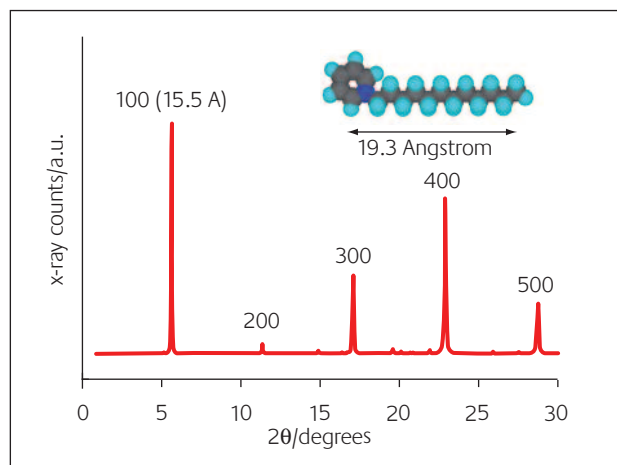
Figure 1
X-ray pattern of 1 with the most prominent reflections.
Inset: estimation of the length of the fully stretched ligand molecule

DSC traces of **1** exhibit an intense exothermic peak between 55 and 120°C on first heating. This is in stark contrast to the corresponding M(II) complexes (M = Co, Ni, Cu, Zn, Cd, Pd),[4-8] which show (endothermic) melting and LC-iso transitions in the DSC. The exothermic peak observed here, however, is similar to DSC traces of mixtures of dodecylpyridinium tetrachlorocuprate and 6-O-palmitoyl ascorbic acid, where the exothermic peak is due to the reduction of Cu(II) to Cu(I) and the formation of CuCl crystals.[12, 13] Here, the exothermic DSC peak is due to the thermal reduction of Au(III) to Au(0).

Optical microscopy confirms the thermal reduction of Au(III) to Au(0) as optical micrographs taken at and above 60°C show the formation of large spherical particles of up to a few micrometers in diameter. Optical microscopy also shows that **1** melts at ca. 50–55°C into a bright yellow liquid.

Gold platelets

Complex **1** can be spin coated, solution cast, or deposited as a powder on various substrates. Atomic force microscopy (AFM) reveals that solution casting yields much rougher films than spin coating. Therefore, we have used dry, crystalline thin films spin coated from THF on glass and mica and dry, crystalline powders of **1** for gold particle fabrication. Both types of samples were irradiated with UV light for various amounts of times and with various lamp-sample distances.

After exposure to UV light the samples exhibit a characteristic chlorine smell, which we assign to the oxidation of Cl$^-$ to Cl$_2$ upon reduction of Au(III) to Au(0). Figure 2 shows that the complex **1** serves as a matrix for the controlled growth of large metallic platelets: after 30 minutes, optical microscopy shows triangular and hexagonal particles with diameters of up to 15 μm in a transparent organic matrix.
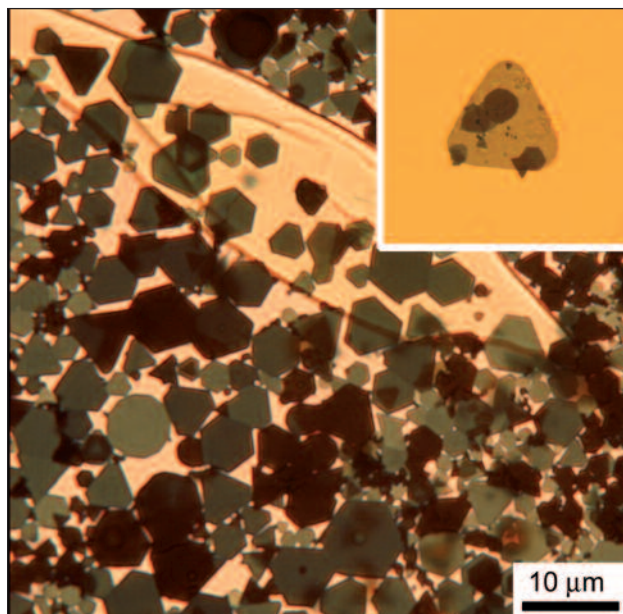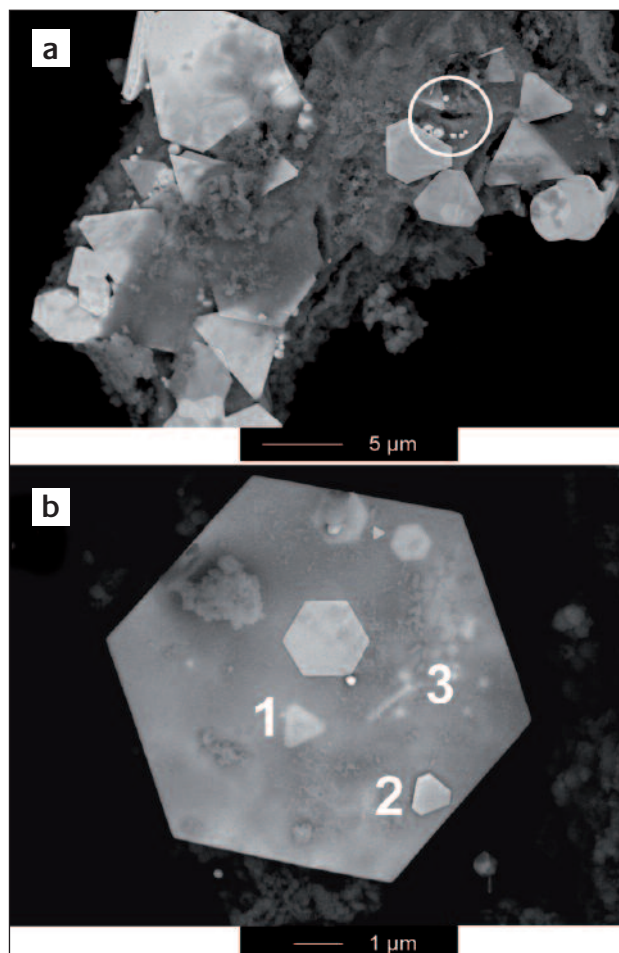

Figure 2

Optical micrograph of gold platelets in the organic matrix after UV irradiation. Inset: large transparent gold particle after extraction. The smaller particles lie below or above the large particle

The particles are often transparent and allow for the observation of particles lying above or below one another. This photochemical fabrication of large platelets from and within the crystalline solid **1** is therefore clearly different from the thermal reduction mentioned above, where only large and roughly spherical particles form.

The formation of the particles is lamp-sample distance dependent. At 43 cm lamp-sample distance, complex **1** is solid and hexagonal platelets like the ones shown in Figure 2, form. At 33 cm, complex **1** is still solid and platelets form, but some spherical particles become visible in the optical microscope. Finally, at 20 cm, complex **1** is a bright yellow liquid within which spherical gold particles of up to several micrometers in diameter appear.

Measurements of the sample temperature find an increasing thermal contribution to particle formation: at 43 and 33 cm, the temperature is roughly 40 to 50°C, whereas at 20 cm the temperature increases up to 70°C. The latter temperature is far above the melting temperature of the complex (ca. 55°C). As a result, at 20 cm lamp-sample

Figure 3

SEM images of gold platelets obtained after 2 hours of UV irradiation: a) low magnification overview over the sample. Besides the large particles visible in the optical microscope, there are also smaller spherical particles (white ring) and some leftover organic matrix. b) Large platelet thin enough to be electron transparent. Some particles lying below (1) and above (2) the large platelet are clearly visible. There is also a particle of ca. 50 nm thickness (3) standing upright beneath the large platelet

distance the reduction of Au(III) takes place in the melt and not in the crystalline state anymore.

The morphological changes from platelet to large spheres show that the temperature at the sample during UV irradiation must be well below the melting transition of the complex **1**, if the formation of gold platelets in a controlled manner is desired. Possibly, cooling of the sample during irradiation or IR filters between lamp and sample will improve the control over particle formation and exclusively yield large hexagonal platelets.

The platelets can be extracted from the organic matrix using dodecanethiol/THF mixtures. The product is a dark red to purple solid and optical microscopy confirms the presence of the platelets, but also shows that some of the organic matrix cannot be removed by washing. The thiols stabilize the particles and the platelets retain their shape even after extended storage.

Figures 3 and 4 are scanning (SEM) and transmission electron microscopy (TEM) images of the particles after extraction. The micrographs show that the particles have a broad size distribution. The width of the platelets ranges from below one to 15 μm. The particles are thin enough to be electron transparent: particles lying below other particles are clearly visible. Typical platelet thicknesses obtained from SEM are between ca. 30 and 100 nm. In TEM, the particles also show bend contours, which are often observed in TEM images of thin metal samples.[19] Furthermore, SEM shows that also smaller particles invisible in the optical microscope form. This is similar to samples obtained by Sun et al.[20] and Li et al.[21] and shows that the dodecylpyridinium matrix does not perfectly control the mineralization. The reason for this behavior is discussed below.

Figure 5 shows an X-ray pattern of **1** after UV irradiation.
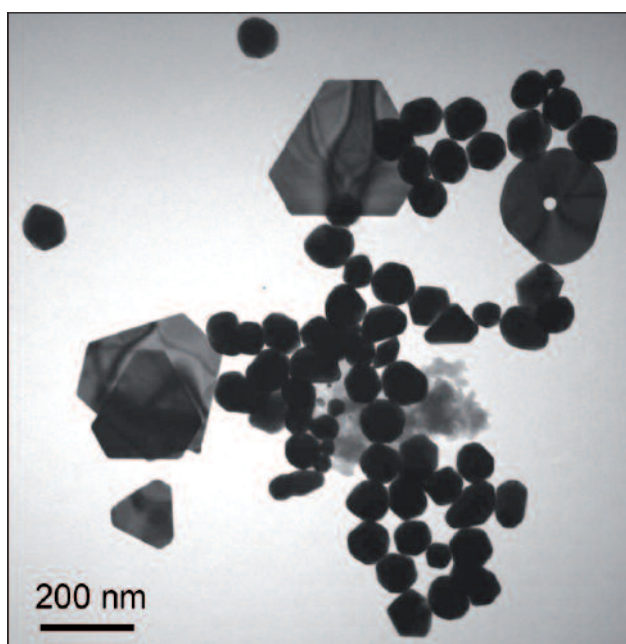
Figure 4

TEM image of a set of smaller platelets and other particles. The dark lines in the platelets are bend contours. The light gray material in the center of the image is some residual organic matrix
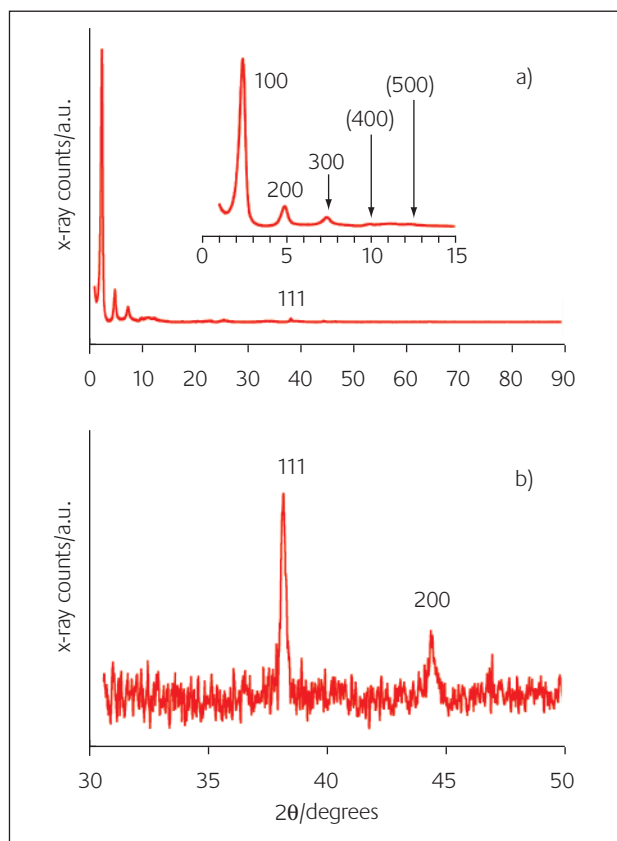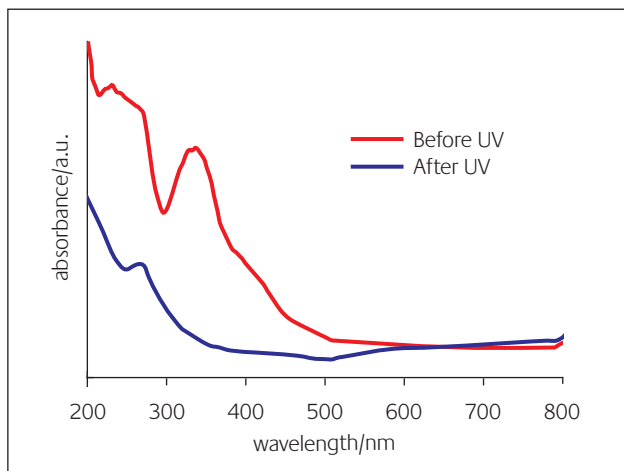

Figure 5

*a) XRD pattern of the complex **1** after 90 minutes of irradiation. The 400 and 500 reflections are barely visible. b) Magnified view of the gold reflections. No other reflection due to gold were found in the X-ray patterns*

At low angles we observe a set of reflections that can be indexed as the 100, 200, 300, and possibly 400 and 500 reflections of a layered structure with a d-spacing of 40 Å. As the dodecyl pyridinium ligand is roughly 19.3 Å long, one interpretation of the 40 Å spacing is a bilayer, possibly from newly formed dodecyl pyridinium chloride. However, the order within this assembly is less perfect than in the crystal of **1**, which can be deduced from the fact that the reflection observed in the X-ray patterns of **1** (Figure 1) are narrower than the reflections of the material after irradiation.

Furthermore, we observe gold 111 and 200 reflections at higher angles. The 111 reflection is most prominent. The fact that the 200 reflection is still visible shows that the sample is not exclusively composed of platelets, as in this case one would see a much stronger 111 reflection and no 200 reflection at all. The X-ray data are thus consistent with electron microscopy, because the electron micrographs clearly show that the control over particle formation is not perfect and some spherical and near-spherical particles form.

Figure 6 shows the UV/Vis spectra of a dry solid film of **1** before UV irradiation and the resulting gold platelet/dodecylpyridinium film after UV irradiation. Complex **1** exhibits a broad band between 212 and 294 nm, a second strong band at 332 nm, and a shoulder at ca. 420 nm. After UV irradiation of a dry film of **1**, the spectrum exhibits a band at 266 nm and an increased absorption from 500 nm to 800
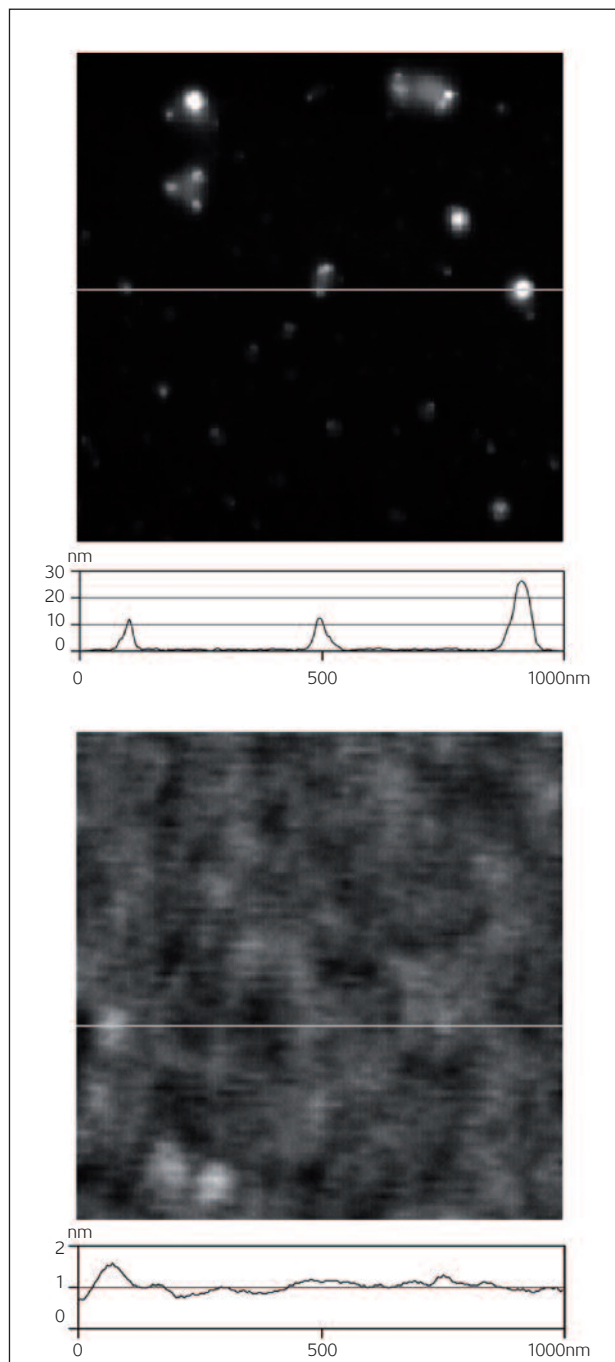
Figure 6

*UV/Vis spectra of dry films of **1** before and after 60 min of UV irradiation. For technical reasons we could not measure the NIR spectra of the samples, even though this spectral region would contain additional information*
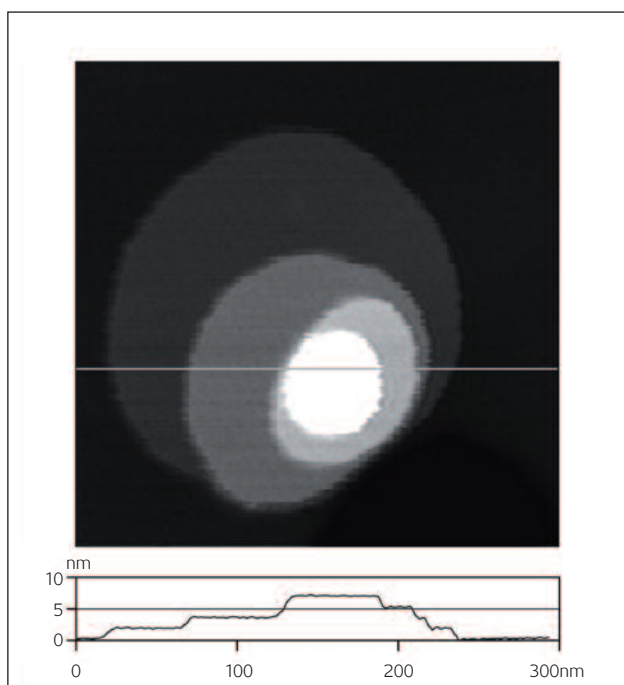
Figure 7

*AFM height image of complex **1** on glass in air (AC mode). The gray line indicates the location of the height profile shown below. Image size is 300 nm x 300 nm. Average step height is 17 ± 1 Å (X-ray layer thickness is 15.5 Å)*

Figure 8

AFM images of two samples irradiated for 90 minutes with a lamp-sample distance of 33 (top) and 43 cm (bottom) showing that the lower sample has a much smoother surfac. Image sizes are 1 μm x 1 μm. Note the different height scale in the line profiles

nm. The spectrum does not show the classical gold colloid surface plasmon band between ca. 400 and 500 nm, which is characteristic for spherical particles. Rather than indicating spherical particles, the UV/Vis spectrum is similar to UV/Vis spectra of gold platelets reported by Sun et al.[20] These authors observe absorption bands at 680 and 925 nm that have been earlier assigned to longitudinal plasmon resonance modes.[22, 23] UV measurements thus show that even though our sample does contain spherical and near-spherical particles, the optical properties are governed by the large platelets.

Particle formation mechanism

To elucidate and possibly optimize the particle formation, we have performed atomic force microscopy (AFM) experiments on the complex **1** and on various irradiated samples. Figure 7 shows that before irradiation, the complex has a flat surface and steps around 17 Å in height. This corresponds well to the layer thickness of 15.5 Å as determined from X-ray scattering (Figure 1).

After 90 minutes of irradiation, we observe a smooth surface. Some steps remain, but their height is now between 38 and 40 Å. We assign this step height again to the layer

height of the newly formed material. The step height distribution is also consistent with a lower order than in the precursor. Both findings are in line with X-ray data, where we found a layer spacing of 40 Å and a less ordered system is indicated by the broad reflections.

Figure 8 illustrates that the lamp-sample distance effect described above is quite strong: at a distance of 33 cm, the surface is smooth. At the same time, we observe a few elevated "peaks" that we assign to (spherical) particles forming within the matrix beneath the sample surface. If the lamp-sample distance increases from 33 cm to 43 cm, the surface is still smooth, but we observe much less of the spherical features.

As stated above, these differences are due to a thermal contribution of the lamp: a shorter lamp-sample distance leads to a temperature increase at the sample and therefore a softening of the template. A softer template will enable the formation of round particles rather than the platelets, which are favored in a more rigid template. Indeed, we have often observed a sticky surface of the samples after irradiation, indicating a softening of the samples upon irradiation. Furthermore, we have observed an increase in the numbers of platelets after increasing the lamp-sample distance by 10 cm to 43 cm. Inversely, if the lamp-sample distance is only 20 cm, the sample melts and we exclusively observe spherical particles with sizes of up to several microns in diameter in the optical microscope.

As a result, we postulate the following growth mechanism: (photo)reduction of the Au(III) ions within the *crystalline* gold complex **1** first leads to Au(0) atoms, which then cluster and form the gold particles. Depending on the temperature of the sample, the organic matrix is softer or stiffer. A stiff matrix (lower temperature at the sample) will predominantly lead to platelets, whereas a soft matrix (higher sample temperature) will not resist the force of the growing gold particles and will not prevent the formation of spherical particles.

Conclusion

Solid-state reactions have been widely explored and exploited in organic chemistry to obtain clearly defined organic compounds, see e.g. refs.[24, 25] However, this is to the best knowledge of the authors one of the first examples showing that inorganic colloids can also form in a solid state reaction from a well-characterized crystalline, molecular precursor, similar to an approach introduced by Chen et al.[17] Solid-state reactions leading to colloidal particles are interesting from a basic scientific point of view but could also be useful for the fabrication of inorganic colloids with new and tunable properties.

We demonstrate here that the presence of an organic template with a long-range order (even though its interaction with the final product is weak) is of crucial importance for the shape control over the observed product. We thus introduce a new approach (photoreduction) for the fabrication of well-

defined inorganic particles from a molecular crystal precursor, which is complementary to the said thermolysis procedure.[17] Our system could for example serve as a template for the fabrication of nanostructured surfaces, because it is soluble in THF and can easily be spin coated on many substrates.

Current efforts are directed towards a better control of the mineralization process, for example by replacing the gold complex **1** with a complex that is more stable with respect to temperature. This should enable us to drive the crystallization more efficiently towards large platelets. Further studies on the fabrication of large nanostructured surfaces are also underway.

Acknowledgements

References

1   M.C. Daniel; D. Astruc, *Chem. Rev.* 2004, **104,** 293

2   M. Antonietti, D. Kuang, B. Smarsly, Y. Zhou, *Angew. Chem. Int. Ed.* 2004, **43,** 4988-4992

3   A. Taubert, *Acta Chim. Slov.* 2005, **52,** 183

4   C.J. Bowlas, D.W. Bruce, K.R. Seddon, *Chem. Commun.* 1996, 1625

5   F. Neve, M. Imperor-Clerc, *Liq. Cryst.* 2004, **31,** 907

6   F. Neve, A. Crispini, S. Armentano, *Chem. Mater.* 1998, **10,** 1904

7   F. Neve, O. Francescangeli, A. Crispini, J. Charmant, *Chem. Mater.* 2001, **13,** 2032

8   F. Neve, O. Francescangeli, A. Crispini, *Inorg. Chim. Acta* 2002, **338,** 51

9   C.K. Lee, H.H. Peng, I.J.B. Lin, *Chem. Mater.* 2004, **16,** 530

10 C. Hardacre; J.D. Holbrey, P.B. McCormac, S.E.J. McMath, M. Nieuwenhuyzen, K.R. Seddon, *J. Mater. Chem.* 2001, **11,** 346

11 K. Binnemans, *Chem. Rev.* 2005, **105,** 4148

12 A. Taubert, P. Steiner, A. Mantion, *J. Phys. Chem.* B 2005, **109,** 15542

13 A. Taubert, *Angew. Chem. Int. Ed.* 2004, **43,** 5380

14 W. Dobbs, J.-M. Suisse, L. Douce, R. Welter, *Angew. Chem. Int. Ed.* 2006, **45,** 4179

15 C.K. Lee, C.S. Vasam, T.W. Huang, H.M.J. Wang, R.Y. Yang, C.S. Lee, I.J.B. Lin, *Organometallics* 2006, **25,** 3768

16 H. Zhu, J.-F. Huang, Z. Pan, S. Dai, *Chem. Mater.* 2006, **18,** 4473

17 Y.-B. Chen, L. Chen, L.-M. Wu, *Inorg. Chem.* 2005, **44,** 9817

18 F. Neve, O. Francescangeli, *Cryst. Growth & Design* 2005, **5,** 163-166

19 D.B. Williams, C.E. Carter, *Transmission Electron Microscopy – A Textbook for Materials Science;* Plenum Press: New York, London, 1996

20 X. Sun, S. Dong, E. Wang, *Angew. Chem. Int. Ed.* 2004, **43,** 6360

21 Z. Li, Z. Liu, J. Zhang, B. Han, J. Du, Y. Gao, T. Jiang, *J. Phys. Chem B* 2005, **109,** 14445

22 S. Link, M.A. El-Sayed, *J. Phys. Chem B* 1999, **103,** 8410

23 S. Link, M.A. El-Sayed, *J. Phys. Chem B* 1999, **103,** 4212

24 L.R. MacGillivray, *Cryst. Eng. Comm.* 2004, **6,** 77

25 H.E. Zimmerman, E.E. Nesterov, *Acc. Chem. Res.* 2002, **35,** 77